

Diameters of Single-Wall Carbon Nanotubes Depending on Helium Gas Pressure in an Arc Discharge

Yahachi Saito* and Yoshihiko Tani

Department of Electrical and Electronic Engineering, Mie University, Tsu 514-8507, Japan

Atsuo Kasuya

Center for Interdisciplinary Research, Tohoku University, Sendai 980-8578, Japan

Received: October 31, 1999; In Final Form: January 6, 2000

Diameter distributions of single-wall carbon nanotubes (SWNTs) produced by an arc discharge with a Rh–Pt catalyst at various helium pressures from 50 to 1520 Torr were studied by transmission electron microscopy and Raman scattering spectroscopy. The distribution shifted systematically to small diameter with the decrease of helium pressure. In addition to the helium pressure, the diameters of SWNTs were dependent on the locations inside the arc evaporator where SWNTs were collected (viz., either on the chamber walls or around the cathode). The most frequently occurring diameters could be controlled from 0.95 nm at 50 Torr to 1.4 nm at 1520 Torr. The effect of helium pressure on the diameters of SWNTs is discussed in connection with the corresponding change in the yield of higher fullerenes.

1. Introduction

Carbon nanotubes have aroused great interest recently because of their unique physical properties, which span a wide range from structural to electronic. For example, nanotubes have a low weight and high elastic modulus, and thus they are predicted to be the strongest fibers.^{1–3} Carbon nanotubes, especially single-wall nanotubes (SWNTs), possess exceptional electronic properties; they can be metallic or semimetallic, depending on the geometry of how a graphene sheet is rolled up into a tube (i.e., diameter and chiral angle).^{4–7} The presence of both metallic and semimetallic nanotubes has been experimentally verified,^{8–10} and quantum properties of electron transport along the nanotubes have been revealed recently.^{11–13} Due to these extreme properties, nanotubes are under investigation in several applications including nanoelectronics devices,^{14,15} electron field emitters,^{16–22} probes of scanning-type microscopes,^{23,24} gas (such as hydrogen) storage materials,^{25,26} and electrode materials of secondary batteries and capacitors.²⁷

To realize these proposed applications, mass production and control of the structures of nanotubes are necessary. So far, relatively large quantities of SWNTs have been produced by using Y–Ni and Fe–Ni catalysts for the electric arc discharge method^{28–30} and by using a Co–Ni catalyst for the pulsed laser ablation method.³¹ Concerning the control of structures (such as diameter and chirality) of SWNTs, it was demonstrated that diameters of SWNTs produced by the arc discharge method can be changed to some extent by selecting metal catalysts; e.g., SWNTs from Fe–Ni have a mean diameter of 1.1 nm, those from Co, 1.3 nm, and those from La, 2.0 nm.³² For the laser ablation method, the diameters of SWNTs can be controlled from 1.0 to 1.3 nm by varying the furnace temperature from 780 to 1200 °C.³³ The chirality of nanotubes, on the other hand, cannot be controlled yet.

In the present study, we found a new method to control the diameters of SWNTs by changing the pressure of helium gas in which the arc discharge was generated. The catalyst used was a mixture of Rh and Pt, which gives a high yield of SWNTs, being comparable with the Y–Ni catalyst. As described in our previous report,³⁴ the Rh–Pt mixture remarkably improves the production of SWNTs compared with the elemental Rh or Pt catalysts.³⁵ The Rh–Pt catalyst has another advantage that both the elements used in the catalyst are nonmagnetic. This enabled us for the first time to measure nuclear magnetic resonance (NMR) spectra of SWNTs even though the metal catalysts were left in the sample.³⁶

2. Experimental Section

The method to produce SWNTs was a dc (direct current) arc discharge between carbon electrodes in helium gas. Figure 1 shows a schematic drawing of the arc evaporator employed in the present experiment. The anode was a graphite rod (6 mm diameter, 50 mm length) in which a hole (3.2 mm diameter, 30 mm deep) was drilled and filled with a mixture of rhodium, platinum, and graphite powders. The mixing ratio of Rh:Pt:C was 5:5:2 by weight. The cathode was a pure graphite rod (13 mm diameter, 30 mm length). The purity of the graphite rod and powder was 99.998%, and the purity of the metal powders was 99.9%.

The pressure of helium gas (purity 99.99%) was varied from 50 to 1520 Torr, and the discharge current was 70 and 100 A, as is listed in Table 1. Since the anode was consumed by evaporation, the arc gap between the electrodes was kept constant, 1–2 mm, by manually advancing the consumed anode. After evaporation for 1–3 min, rubbery soot was obtained around the cathode (indicated by arrow A in Figure 1) and on the inner wall of the reaction chamber (arrow B in Figure 1). These soot materials were individually collected from the respective regions. Hereafter, we call the soot grown around the cathode (A in Figure 1) “cathode soot”, and that on the

* To whom correspondence should be addressed. E-mail: saito@is.elec.mie-u.ac.jp.

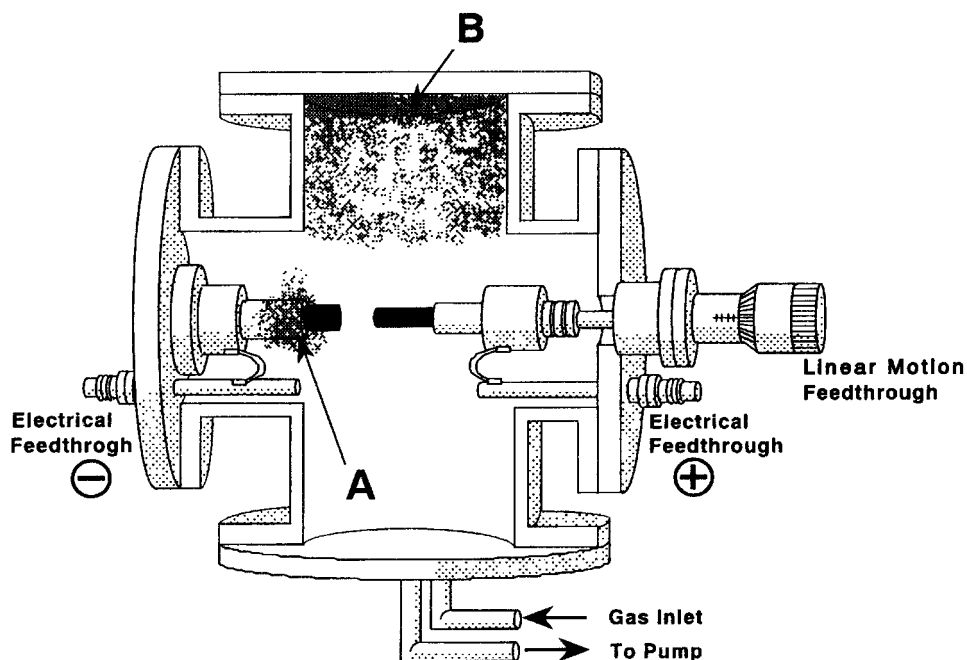


Figure 1. Schematic drawing of the dc arc evaporator used for producing single-wall carbon nanotubes. Soot grown around the cathode surfaces (indicated by arrow A) and that on the inner wall of the evaporator (arrow B) were separately collected.

TABLE 1: Densities of SWNTs in Crude Soot Obtained from Rh–Pt Catalyst at Various Helium Pressures

He pressure (Torr)	arc current (A)	density of SWNTs ^a	
		cathode soot	chamber soot
50	70	very low	very low
50	100	low	very low
100	100	low	very low
300	100	medium	low
600	70	high	low
600	100	very high	low
1520	100	low	no

^a Densities in raw soot are graded into five classes: very high (more than 50%), high (~30%), medium (~10%), low (~1%), very low (less than 1%). In the estimation of the SWNT density, metal catalysts are excluded.

inner wall of the reaction chamber (B in Figure 1) “chamber soot”. For the chamber soot, we collected samples only from those deposited on the ceiling of the chamber.

Recovered soot materials were examined by transmission electron microscopy (TEM), Raman scattering spectroscopy, and X-ray diffraction (XRD). For preparing samples for TEM, soot materials were dispersed in ethanol under ultrasonic agitation. The suspension was dropped on holey carbon grids and allowed to dry. A transmission electron microscope (Philips CM120) was operated at 120 kV. Raman scattering spectra were measured in a backscattering geometry at room temperature using an Ar ion laser (488 nm). XRD was performed with a powder X-ray diffractometer with a Cu K α source.

3. Results

The abundance of SWNTs produced under various preparation conditions is summarized in Table 1. The density of SWNTs was estimated by TEM observation and Raman scattering. The density of SWNTs was higher in the cathode soot than in the chamber soot. The yield of SWNTs was strongly dependent on the helium pressure. The electric current of the arc discharge also affected the yield of SWNTs though its effect was not as serious as the helium pressure. The highest yield of SWNTs

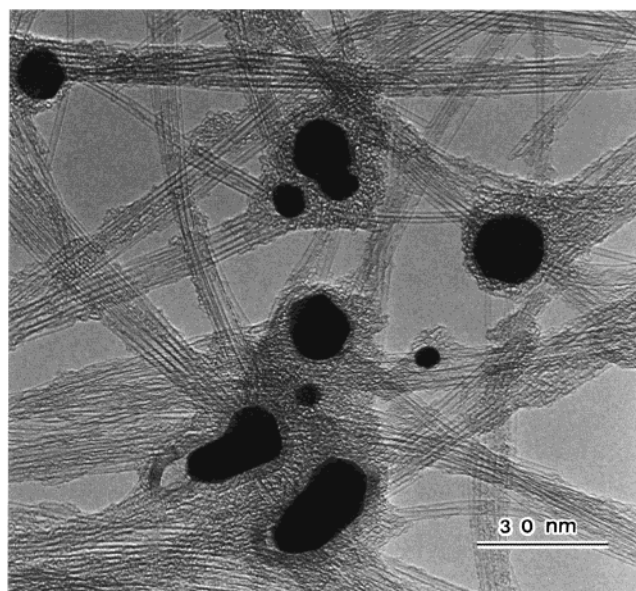


Figure 2. TEM picture of SWNTs grown around the cathode surfaces at 600 Torr of helium. Dark, spherical particles are Rh–Pt alloy particles.

was obtained at 600 Torr of helium and with 100 A of arc current.

Figure 2 shows a typical TEM picture of SWNTs in the cathode soot prepared at the optimum conditions (giving the highest yield). SWNTs are entangled with each other, exhibiting “highway-junction”-like patterns. The length of SWNTs exceeds 10 μ m. Not only bundles but also isolated SWNTs are observed. Similar growth morphology is commonly observed for samples containing long SWNTs with a high density, e.g., soot samples obtained from Y–Ni and Fe–Ni catalysts, which are known to be the most efficient catalysts for yielding SWNTs by arc evaporation.^{28–30} In the as-grown soot, the sizes of the bundles are small; i.e., the number of SWNTs forming a bundle is only a few to 10, while the bundle size grows after the purification process.^{37,38}

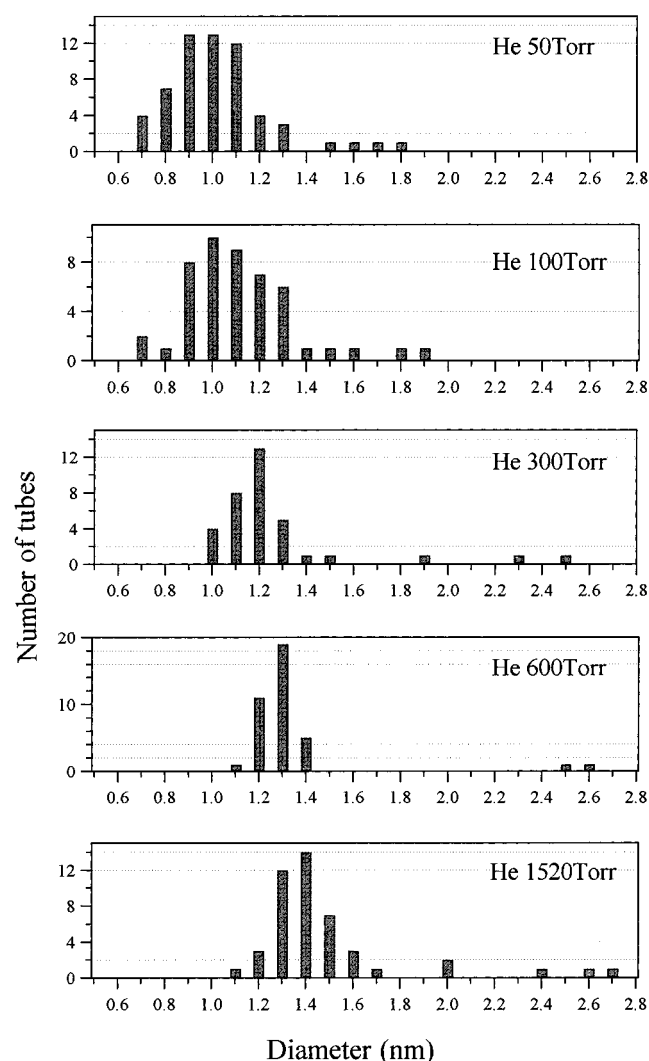


Figure 3. Histograms of the diameters of SWNTs in the cathode soot at 50, 100, 300, 600, and 1520 Torr of helium.

Dark, spherical particles with diameters of 10–20 nm observed in Figure 2 were Rh–Pt alloys with a fcc structure, as revealed by electron diffraction and XRD. The composition of alloy particles was estimated to be Rh–54 atom % Pt from the measured lattice constant ($a = 0.386$ nm).

Diameters of SWNTs prepared under various pressures were measured with TEM. In Figures 3 and 4 are shown diameter distributions of SWNTs in the cathode and the chamber soot, respectively. It is found that the distributions of SWNT diameters shift systematically with the change of helium pressure for both the cathode and the chamber soot; the lower the helium pressure, the smaller the diameter. Mode diameters (i.e., most frequently occurring diameters) vary from 0.95 nm at 50 Torr to 1.4 nm at 1520 Torr for the cathode soot, and from 1.0 nm at 50 Torr to 1.4 nm at 600 Torr for the chamber soot. In Figure 5, the mode diameters are plotted as a function of the logarithm of helium pressure for both the cathode and the chamber soot. A nearly linear relation between the diameter and the log of helium pressure is found though the reason is not known. In addition to the obvious pressure dependence of the diameters, a difference in the mean diameters between the cathode and the chamber soot is clearly found. The diameters of SWNTs in the cathode soot were always smaller than those in the chamber soot.

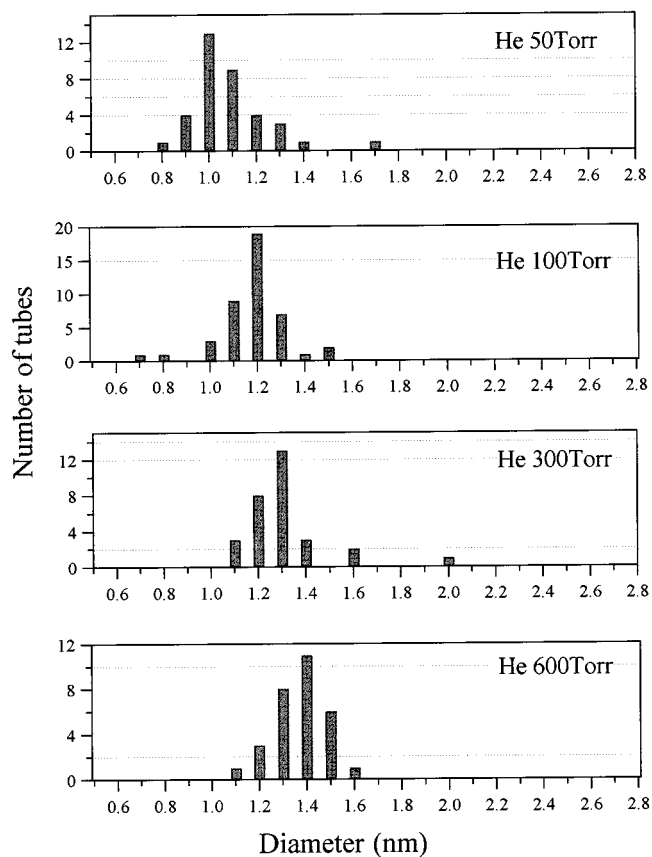


Figure 4. Histograms of the diameters of SWNTs in the chamber soot at 50, 100, 300, and 600 Torr of helium.

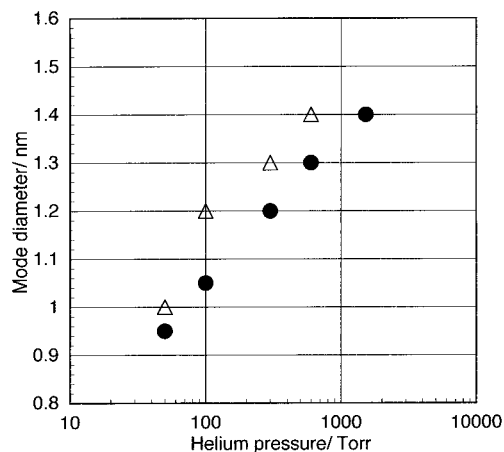


Figure 5. Mode diameters (most frequently occurring diameter) of SWNTs versus the logarithm of the helium pressure, exhibiting a nearly linear relation. SWNTs in the cathode are represented by solid circles, and those in the chamber soot by open triangles.

Raman scattering spectra in a low-frequency region of so-called “breathing modes” of SWNTs also revealed the pressure dependence of SWNT diameters, as shown in Figure 6. The spectra in parts a and b of Figure 6 were obtained from the cathode soot prepared at 50 and 600 Torr, respectively, with laser excitation at 488 nm. SWNTs grown at 50 Torr give larger Raman shifts compared with those grown at 600 Torr. Since the Raman shift of the breathing mode is inversely proportional to the tube diameter,^{39,40} the large Raman shifts observed for the low helium pressure indicate small diameters of nanotubes. The Raman spectrum of SWNTs grown at 50 Torr (Figure 6a) exhibits several peaks in a range from 180 to 260 cm^{-1} . This

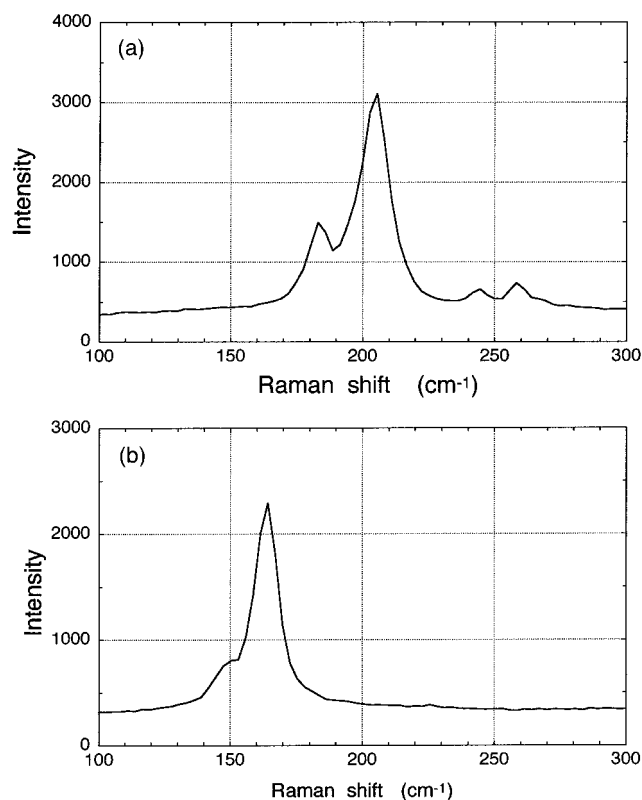


Figure 6. Raman scattering spectra in the low-frequency region of so-called breathing modes of SWNTs. Spectra a and b were obtained from as-prepared SWNTs grown in cathode soot at helium pressures of 50 and 600 Torr, respectively.

frequency range corresponds to diameters of SWNTs from 0.8 to 1.23 nm. On the other hand, the Raman spectrum for 600 Torr (Figure 6b) is dominated by a peak at 167 cm^{-1} accompanying a small hump around 185 cm^{-1} , indicating a narrow distribution of diameters from 1.20 to 1.35 nm. These Raman spectra are consistent with the diameter distributions measured by TEM (see Figure 3).

The present study shows that the tube diameters can be controlled by varying the helium pressure though the yield of SWNTs is affected by the pressure at the same time. At the highest yield of SWNTs, the diameter distribution is the narrowest and has a peak at 1.3 nm. This value of the diameter is close to that for the (10, 10) tube. Other catalysts, Y–Ni and Fe–Ni, gave similar relation between the yield and the diameter of SWNTs; i.e., when the yield of SWNTs was the highest, the most frequently occurring diameter was around 1.3 nm.⁴¹

4. Discussion

4.1 Correlation between SWNT Diameters and Fullerene Sizes. Relevant to the pressure-dependent diameter of SWNTs found in the present study, it should be noted that the size of fullerenes produced by an arc discharge is also dependent on the helium pressure. It is known that the yield of higher fullerenes such as C_{72} and C_{84} increases with an increase in the helium pressure.^{42,43} The positive correlation in the diameter between SWNTs and fullerenes indicates that the sizes of closed carbon networks increase with the increase in the environmental gas pressure, and furthermore suggests that the growths of both forms of carbon (i.e., SWNT and fullerene) are correlated with each other.

For laser vaporization, diameters of SWNTs can be varied by controlling the temperature of the carrier gas; the most

frequent tube diameter shifts from 1.0 to 1.22 nm as the temperature increases from 780 to 1000 °C.³³ In parallel with this phenomenon, it was also reported that the yield of higher fullerenes (from C_{76} to C_{96}) increased with increasing temperature of the carrier gas.⁴⁴ Again, the correlation in sizes of both forms of carbon is found in the laser vaporization, where the temperature of the ambient gas is the key parameter.

In the arc method, the temperature and the gas pressure in a growth region of carbon clusters cannot be controlled independently. However, the pressure dependence of SWNT diameters and fullerene sizes observed in the arc method coincides with their temperature dependence found in the laser vaporization method. This suggests that the increase in gas pressure in the arc evaporation method has an effect of raising the temperature in the nucleation and growth region around the arc gap. This pressure effect on the gas temperature may be qualitatively explained as follows. At high ambient pressure, the diffusion of hot vapor around the arc gap is restricted and the vapor is confined to a narrow region near the evaporation source. Thus, nucleation of carbon vapor occurs at high temperature when the pressure of the gas is high.

Then we have to address the question of why larger SWNTs and fullerenes grow at higher temperature. Achiba and his group⁴⁴ pointed out that there might exist an activation barrier against the formation of closed fullerene structures and that the activation energy might be higher for the higher fullerenes. This may hold for SWNTs; i.e., the larger the diameter of SWNTs, the higher the activation barrier, because the higher temperature is required for the formation of the thicker SWNTs. According to our model of SWNT growth previously proposed,^{45,46} the caps of SWNTs are first formed on the surface of catalytic particles, and then carbon atoms are supplied to the roots of the caps, and tubular structures are formed. This root growth model implies that the diameter of a SWNT is determined by the diameter of the initial hemispherical cap. The diameters of both the hemispherical caps and fullerenes depend on the concentration of pentagons in the hexagonal network; the higher the pentagon concentration, the smaller the diameters. We believe that the activation barriers against the formation of larger fullerenes and thicker SWNTs correspond to the conversion of pentagons in a carbon cluster to hexagons. When the pentagons formed are rapidly converted to hexagons, larger caps and fullerenes are produced. At higher temperature, the pentagons can be annealed to hexagons with the addition of condensing carbon atoms to the growth nuclei.

4.2. Diameters of SWNTs at the Highest Yield. It has been reported that the laser evaporation technique with a Co–Ni catalyst produces SWNTs with a very high yield of over 70%.³¹ The diameters of SWNTs produced by the laser evaporation are reportedly to be 1.36 nm corresponding to that of the (10, 10) tube.³¹ The laser method as well as the present arc method produced SWNTs with a diameter of around 1.3 nm when the yield of SWNTs was the highest. The reason is not clear at present, though the coincidence between the two preparation methods concerning the yield and the diameters of SWNTs seems to indicate that it is the thermodynamic stability rather than growth kinetics that brings about the selective formation of SWNTs with diameters of around 1.3 nm.

5. Conclusion

Using the arc discharge method with the binary Rh–Pt catalyst, we demonstrated that the diameter of SWNTs could be controlled from 0.95 to 1.4 nm by changing the helium pressure in the arc chamber. The present finding will be applied

to prepare SWNT samples with desired diameters, which should enable us to explore the diameter-dependent properties of SWNTs, and also shed light on the growth mechanism of SWNTs.

Acknowledgment. This work was partially supported by the Ministry of Education, Science, Sports and Culture of Japan (Grants-in-Aid for Scientific Research on the Priority Area "Fullerenes and Nanotubes") and by the NEDO project "Frontier Carbon Technology".

References and Notes

- (1) Treacy, M. M. J.; Ebbesen, T. W.; Gibson, J. M. *Nature* **1996**, *381*, 678.
- (2) Iijima, S.; Brabec, C.; Maiti, A.; Bernholc, J. *J. Chem. Phys.* **1996**, *104*, 2089.
- (3) Falvo, M. R.; Clary, G. J.; Taylor, R. M., II; Chi, V.; Brooks Jr., F. P.; Washburn, S.; Superfine, R. *Nature* **1997**, *389*, 582.
- (4) Mintmire, J. M.; Dunlap, B. I.; White, C. T. *Phys. Rev. Lett.* **1992**, *68*, 631.
- (5) Hamada, N.; Sawada, S.; Oshiyama, A. *Phys. Rev. Lett.* **1992**, *68*, 1579.
- (6) Saito, R.; Fujita, M.; Dresselhaus, G.; Dresselhaus, M. S. *Appl. Phys. Lett.* **1992**, *60*, 2204.
- (7) Tanaka, K.; Okahara, K.; Okada, M.; Yamabe, T. *Chem. Phys. Lett.* **1992**, *191*, 469.
- (8) Wildoer, J. W. G.; Venema, L. C.; Rinzler, A. G.; Smalley, R. E.; Dekker, C. *Nature* **1998**, *391*, 59.
- (9) Odom, T. W.; Huang, J.-L.; Kim, P.; Lieber, C. M. *Nature* **1998**, *391*, 62.
- (10) Sugano, M.; Kasuya, A.; Tohji, K.; Saito, Y.; Nishina, Y. *Chem. Phys. Lett.* **1998**, *292*, 575.
- (11) Tan, S. J.; Devoret, M. H.; Dai, H.; Thess, A.; Smalley, R. E.; Greerlign, L. J.; Dekker, C. *Nature* **1997**, *386*, 474.
- (12) Frank, S.; Poncharal, P.; Wang, Z. L.; De Heer, W. A. *Science* **1998**, *280*, 1744.
- (13) Venema, L. C.; Wildoer, J. W. G.; Janssen, J. W.; Tans, S. J.; Tuinstra, H. L. J. T.; Kouwenhoven, L. P.; Dekker, C. *Science* **1999**, *283*, 52.
- (14) Hu, J.; Ouyang, M.; Yang, P.; Lieber, C. M. *Nature* **1999**, *399*, 48.
- (15) Zhang, Y.; Ichihashi, T.; Landree, E.; Nihey, F.; Iijima, S. *Science* **1999**, *285*, 1719.
- (16) Rinzler, A. G.; Hafner, J. H.; Nikolaev, P.; Lou, L.; Kim, S. G.; Tomanek, D.; Nordlander, P.; Colbert, D. T.; Smalley, R. E. *Science* **1995**, *269*, 1550.
- (17) De Heer, W. A.; Chatelain, A.; Ugarte, D. *Science* **1995**, *270*, 1179.
- (18) Saito, Y.; Hamaguchi, K.; Hata, K.; Uchida, K.; Tasaka, Y.; Ikazaki, F.; Yumura, M.; Kasuya, A.; Nishina, Y. *Nature* **1997**, *389*, 554.
- (19) Saito, Y.; Uemura, S.; Hamaguchi, K. *Jpn. J. Appl. Phys.* **1998**, *37*, L346.
- (20) Wang, Q. H.; Setlur, A. A.; Lauerhaas, J. M.; Dai, J. Y.; Seeling, E. W.; Chang, R. P. H. *Appl. Phys. Lett.* **1998**, *72*, 2912.
- (21) Choi, W. B.; Chung, D. S.; Park, S. H.; Kim, J. M. *Proceedings of SID '99*; p 1134.
- (22) Uemura, S.; Yotani, J.; Nagasako, T.; Saito, Y.; Yumura, M. *Proceedings of Euro Display '99 (19th IDRC)*; p 93.
- (23) Dai, H.; Hafner, J. H.; Rinzler, A. G.; Colbert, D. T.; Smalley, R. E. *Nature* **1996**, *384*, 147.
- (24) Wong, S. S.; Joselevich, E.; Woolley, A. T.; Cheung, C. L.; Lieber, C. M. *Nature* **1998**, *394*, 52.
- (25) Dillon, A. C.; Jones, K. M.; Bekkedahl, T. A.; Kiang, C. H.; Bethune, D. S.; Haben, M. J. *Nature* **1997**, *386*, 377.
- (26) Chen, P.; Wu, X.; Lin, J.; Tan, K. L. *Science* **1999**, *285*, 91.
- (27) Gao, B.; Kleinhammes, A.; Tang, X. P.; Bower, C.; Fleming, L.; Wu, Y.; Zhou, O. *Chem. Phys. Lett.* **1999**, *307*, 153.
- (28) Seraphin, S.; Zhou, D. *Appl. Phys. Lett.* **1994**, *64*, 2087.
- (29) Saito, Y.; Koyama, T.; Kawabata, K. *Z. Phys. D* **1997**, *40*, 421.
- (30) Journet, C.; Maser, W.; Bernier, P.; Loiseau, A.; Chapelle, M. L.; Lefrant, S.; Deniard, P.; Lee, R.; Fischer, J. E. *Nature* **1997**, *388*, 756.
- (31) Thess, A.; Lee, R.; Nikolaev, P.; Dai, H.; Petit, P.; Robert, J.; Xu, C.; Lee, Y. H.; Kim, S. G.; Rinzler, A. G.; Colbert, D. T.; Scuseria, G. E.; Tomanek, D.; Fischer, J. E.; Smalley, R. E. *Science* **1996**, *273*, 483.
- (32) Kasuya, A.; Sasaki, Y.; Saito, Y.; Tohji, K.; Nishina, Y. *Phys. Rev. Lett.* **1997**, *78*, 4434.
- (33) Bandow, S.; Asaka, S.; Saito, Y.; Rao, A. M.; Grigorian, L.; Richter, E.; Eklund, P. C. *Phys. Rev. Lett.* **1998**, *80*, 3779.
- (34) Saito, Y.; Tani, Y.; Miyagawa, N.; Mitsushima, K.; Kasuya, A.; Nishina, Y. *Chem. Phys. Lett.* **1998**, *294*, 593.
- (35) Saito, Y.; Nishikubo, K.; Kawabata, K.; Matsumoto, T. *J. Appl. Phys.* **1996**, *80*, 3062.
- (36) Ogata, H.; Bandow, S.; Kuno, S.; Saito, Y. Presented at the Materials Research Society 1999 Fall Meeting, Boston, Nov 29 to Dec 3, 1999; Paper U3.4.
- (37) Tohji, K.; Goto, T.; Takahashi, H.; Shinoda, Y.; Shimizu, N.; Jeyadevan, B.; Matsuoka, I.; Saito, Y.; Kasuya, A.; Ohsuna, T.; Hiraga, K.; Nishina, Y. *Nature* **1996**, *383*, 679.
- (38) Tohji, K.; Takahashi, H.; Shinoda, Y.; Shimizu, N.; Jeyadevan, B.; Matsuoka, I.; Saito, Y.; Kasuya, A.; Ito, S.; Nishina, Y. *J. Phys. Chem. B* **1997**, *101*, 1974.
- (39) Jishi, R. A.; Inomata, D.; Nakao, K.; Dresselhaus, M. S.; Dresselhaus, G. *J. Phys. Soc. Jpn.* **1994**, *63*, 2252.
- (40) Rao, A. M.; Richter, E.; Bandow, S.; Chase, B.; Eklund, P. C.; Williams, K. A.; Fang, S.; Subbaswamy, K. R.; Menon, M.; Thess, A.; Smalley, R. E.; Dresselhaus, G.; Dresselhaus, M. S. *Science* **1997**, *275*, 187.
- (41) Tani, Y.; Saito, Y. Unpublished data.
- (42) Saito, Y.; Inagaki, M.; Shinohara, H.; Nagashima, H.; Ohkohchi, M.; Ando, Y. *Chem. Phys. Lett.* **1992**, *200*, 643.
- (43) Achiba, A.; Wakabayashi, T.; Morikawa, T.; Suzuki, S.; Shiromaru, H. *Mater. Sci. Eng., B* **1993**, *19*, 14.
- (44) Kasuya, D.; Ishigaki, T.; Suganuma, T.; Ohtsuka, Y.; Suzuki, S.; Shiromaru, H.; Achiba, Y.; Wakabayashi, T. *Eur. J. Phys. D*, in press.
- (45) Saito, Y.; Okuda, M.; Fujimoto, N.; Yoshikawa, T.; Tomita, M.; Hayashi, T. *Jpn. J. Appl. Phys.* **1994**, *33*, L526.
- (46) Saito, Y.; Okuda, M.; Tomita, M.; Hayashi, T. *Chem. Phys. Lett.* **1995**, *236*, 419.